Interactions (2024) 245:73
https://doi.org/10.1007/s10751-024-01910-4

CONFERENCE PROCEEDING

Structural, electronic, and magnetic properties of pyrochlore $Nd_2Ir_2O_7$ studied by first-principles calculations

Supparat Charoenphon[1,2] · Utami Widyaiswari[5] · Muhammad Abdan Syakuur[4] · Retno Asih[3] · Pakpoom Reunchan[2] · Isao Watanabe[1,2]

Accepted: 10 April 2024
© The Author(s), under exclusive licence to Springer Nature Switzerland AG 2024

Abstract
First-principle calculations have been performed on the Nd-based pyrochlore iridate, $Nd_2Ir_2O_7$, to investigate electronic structures and magnetic properties. The generalized gradient approximation formalism, GGA, has been used to correct the string onsite Coulomb repulsion energy (U) between localized $5d$ and $4f$ electrons. Our present study found that combinations of U value on Nd, U_f, and Ir, U_d affect the electronic and magnetic properties of $Nd_2Ir_2O_7$. Setting U_f and U_d to be 5 eV for each, the all-in-all-out (AIAO) magnetic spin structure gives rise to a small Ir^{4+} magnetic moment of 0.37 μ_B and Nd^{3+} magnetic moment of 3.00 μ_B, a band gap of $Nd_2Ir_2O_7$ was estimated to be 1.50 eV starting to open a sizable band gap to change the system from metal to insulator and stable in ferromagnetic phase.

Keywords First principle calculation · Pyrorochlore iridate

1 Introduction

Neodymium-based iridate, $Nd_2Ir_2O_7$, attract great interest due to combinations of characters between the strong spin-orbit coupling (SOC) and electron-electron interactions [1–5], which lead to a variety of intriguing cooperative phenomena such as a metal-insulator transition

✉ Supparat Charoenphon
supparat.charoenphon@riken.jp

Isao Watanabe
nabedon@riken.jp

1 Meson Science Laboratory, RIKEN Nishina Center, 2-1 Hirosawa, Wako, Saitama 351-0198, Japan

2 Department of Physics, Faculty of Science, Kasetsart University, Bangkok 10900, Thailand

3 Department of Physics, Faculty of Mathematics and Natural Science, Institut Teknologi Sepuluh Nopember, Surabaya 60111, Indonesia

4 Department of Chemistry, Faculty of Mathematics and Natural Sciences, Padjadjaran University, Jatinangor, Sumedang 45363, Indonesia

5 Department of Physics, Faculty of Mathematics and Natural Sciences, Padjadjaran University, Jatinangor, Sumedang 45363, Indonesia

Published online: 20 April 2024

(MIT) [6], unconventional superconductivity [7, 8], magnetoelectric effect [9, 10] and Weyl semimetal [11]. The $Nd_2Ir_2O_7$ has the geometrical frustration caused by the corner-shared pyrochlore lattice, leading to unique magnetic interactions between $4f$ electrons of rare earth ions and $5d$ electrons of transition metals [12]. This magnetic fructration based on the pyrochlore lattice is a key factor in generating magnetic ground state $Nd_2Ir_2O_7$.

Recently, it was reported that the family of R_2Ir_2O compounds showed a systematic decrease in the MIT temperature with increasing in the ionic radius of R, reaching zero between Nd to Pr [13–15]. A subtle interplay influenced by factors like the lattice stoichiometry and possible impurities. Initially, $Nd_2Ir_2O_7$ was reported to be metallic at all temperatures [16]. With improving the sample quality, and optical conductivity study reported the apperence of MIT at 37 K [14] with the energy gap E_g of about 45 meV [17]. The resistivity slightly increased under pressure below 20 K at MIT [18]. A magnetic order associated to MIT was reported as well and expected to be the ferromagnetic one by Nd^{3+} moments [19]. Neutron diffraction studies suggest that both the Ir^{4+} and the Nd^{3+} moments have an all-in all-out (AIAO) magnetic structure with magnetic moments of 0.34 μ_B and 1.27 μ_B at 1.8 K, respectively [20]. On the other hand, other studies reported that $Nd_2Ir_2O_7$ showed an antiferromagnetic long-range order with the propagation vector, q_0, of (0,0,0), with magnetic moments of 2.3 ± 0.4 μ_B for Nd and 0.2 μ_B for Ir [19]. Each study struggled with models and was unable to confirm the ground state of $Nd_2Ir_2O_7$ correctly.

The Density Functional Theory (DFT) calculation is a good technique in studying materials when the on-site Coulomb potential energy, U, and SOC should be considered to estimate the electronic and magnetic properties because it has been demonstrated in our previous paper that GGA was a suitable function to describe electronic states of strongly correlated system rather than LDA or PBE [21], and also because it is well known that Ir atom has a strong SOC generally [22, 23]. $Nd_2Ir_2O_7$ has been known to be beyond the applicability of LDA+U calculations and overestimated the stability of insulating magnetically ordered states and U. We have simply tested LDA+U already before the current study and found that LDA+U. Actually, LDA+SOC+U predicted that $Y_2Ir_2O_7$ could host nontrivial Weyl semimetal and axion insulator phases. This extended method succeeded to explain the phase diagram of $Y_2Ir_2O_7$ with the the AIAO ground-state configuration of Ir magnetic moments. While GGA+SOC calculations reported a metallic ground state in $Y_2Ir_2O_7$ and $Pr_2Ir_2O_7$ but insulating in $Eu_2Ir_2O_7$ opening a band gap, GGA+SOC+U calculations showed a semimetallic ground state in $Pr_2Ir_2O_7$ and opened a sizeable band gap in $Y_2Ir_2O_7$ and $Eu_2Ir_2O_7$ to be insulators [24]. The DFT and dipole-field calculations of $Nd_2Ir_2O_7$ report the magnetic moments of Ir and Nd were estimated to be 0.12 and Nd 0.20 μ_B [25], respectively, less than the experiment value. This is a good example to describe how LDA is insufficient to describe the electric state of the strongly correlated system. Accordingly, treatments of the electronic correlations by SOC and GGA are important to shed light on MIT in pyrochlore iridates. In this study, we aimed to clarify the electronic state of $Nd_2Ir_2O_7$ from Metal to be in insulator and magnetics moment of Nd and Ir by using DFT calculations reproduce experimental results as much as possible. We used GGA+SOC+U to investigate how structural and electronic properties were affected by changing U systematically on Nd and Ir, determining the ground state of $Nd_2Ir_2O_7$. This kind of systematic DFT study on pyrochlore iridate adjusting U and SOC has not been studied previously. We tested several values of U, ranging from 0 to 8 eV calculating the lattice parameters, band gap, and total magnetic moment of Nd and Ir in this study.

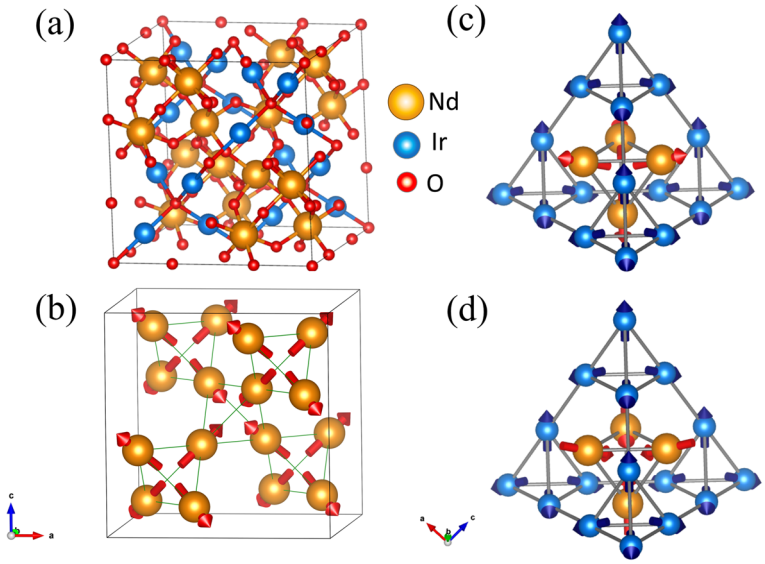

Fig. 1 (a) An illustration of $Nd_2Ir_2O_7$ cubic cell containing 88 atoms and the its local atomic structure (b) Model of All-in all-out magnetic structure of $Nd_2Ir_2O_7$. The orange balls represent Nd^{3+} ions, and the red arrows represent the direction of Nd magnetic moments. (c) Ferromagnetic relation of magnetic moments between Ir (blue balls) and Nd (orange balls). Both the Ir and the Nd magmetic moments form the all-in all-out structures. (d) Antiferromagnetic relation of magnetic moment between Nd and Ir

2 Methodology

Our DFT calculations employed the Generalized Gradient Approximation scheme (GGA) [26]. The pseudopotential projector augmented wave (PAW) method for electron-ion interactions was implemented in Vienna ab-initio Simulation Package (VASP). We used the well-converged energy cut-off of 400 eV for the projected-augmented plane waves. The standard Duradev implementation for DFT+U calculations was used with the effective onsite Coulomb interaction for localized orbitals parametrized, $U_{eff} = U - J$ (The U_{eff} denotes henceforth as U_d and U_f) [27]. We set J=0. The SOC effect was set on Nd atom. The simple unit cell with the space group of Fd-3m encompassed 88 atoms and was used in all calculations [28]. The lattice parameter and ionic positions were calculated self-consistently until the residual forces were smaller than 0.02 eV with an energy convergence criterion of 10^{-5} eV. For the calculations of lattice parameters and band gaps, we employed a 22-atom primitive cell with $7\times7\times7$ Monkhorst-Pack (MP) meshes for the Brillouin zone integrations. For the calculations, the magnetic moment of Ir and Nd and various magnetic configurations, such as non-magnetism (NM), ferromagnetic (FM), and antiferromagnetic (AFM), with SOC effect on Nd, we use supercell 88-atoms with the Brillouin zone integrations of the supercell, the k-points were sampled at a non-Γ-centered MP $2\times2\times2$ mesh. The computational lattice model for $Nd_2Ir_2O_7$ is shown in Fig. 1a.

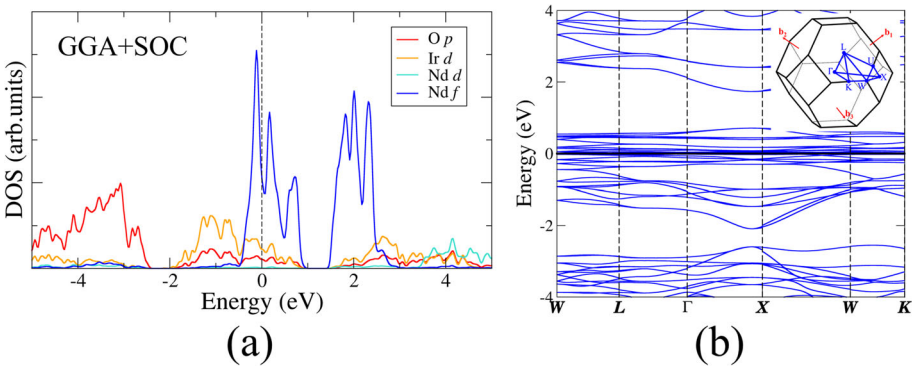

Fig. 2 The GGA+SOC calculated projected density of states (PDOS), (b) Electronic band structure of $Nd_2Ir_2O_7$ show the first Brillouin zone with the path W-L-Γ-X-W-K [29]

3 Electronic and magnetic structure

$Nd_2Ir_2O_7$ structure in the cubic Fd-3m space group is shown in Fig. 1a. The structure is three-dimensional. Nd^{3+} is bonded in a distorted body-centered cubic geometry to eight O^{2-} atoms. There are two shorter (2.27 Å) and six longer (2.55 Å) Nd-O bond lengths. Ir^{4+} is bonded to six equivalent O^{2-} atoms to form corner-sharing IrO_6 octahedra. All Ir-O bond lengths are 2.04 Å. The filled circles represent Nd^{3+} ions, and the arrows represent the Nd moments shown in Fig. 1b. The magnetic possibility of $Nd_2Ir_2O_7$, Both the Ir and the Nd moments form the AIAO structures. Alternative directions of Nd moments in the case of a ferromagnetic Nd-Ir interaction are depicted as shown in Fig. 1c. In contrast, the moments are antiferromagnetic as shown in Fig. 1d, the directions of all the red arrows are reversed. Figure 2 shows the Density of the state and the band structure in the GGA+SOC approximation. The O-p states are mostly less than -2.5 eV below the Fermi level, and a little cluster contributed near the Fermi energy. The occupied part of Ir-d states is found from -1.9 eV to -0.8 eV and 1.8 eV to 4.4 eV energy interval and has some parts overlapped with O-p and Nd-f states. The Nd-f states have contributed more near the Fermi energy from -0.5 eV to 0.9 eV and 1.5 eV to 2.8 eV. There is also a small contribution from Nd-d states in the valence band. Our calculated band gap is no band gap and produces a metallic ground state in $Nd_2Ir_2O_7$ in contradiction with resistivity measurements which claim that $Nd_2Ir_2O_7$ is a Mott insulator. In the next section, we use the GGA+SOC+U method to produce the insulating ground state and correctly the magnetic ground state in $Nd_2Ir_2O_7$.

3.1 $U_d \neq 0, U_f = 0$

Firstly, we set U_d on only Ir atoms. The U_d varied between 0 and 8 eV and influenced the energy levels of the d orbital on the Ir atom of $Nd_2Ir_2O_7$. Figure 2 presents the total and partial density of states (PDOS) of $Nd_2Ir_2O_7$ in the GGA+SOC+U approximation. The GGA+SOC+U approximation showed that the O-p and Ir-d states have more contributions around Fermi energy, starting from $U_d = 0$ to 3 eV. Then, the O-p and Ir-d were spread out at $U_d = 4$ eV and decreased around 0.6 eV over a U_d range from 5 to 7 eV. The 5d orbital in Ir hybridizes strongly with the O-2p orbital. Their relative energetic position determines the degree of hybridization and the width of the valence band. As the occupied 5d states

Table 1 Calculated lattice parameters (a) and magnetic moment of Ir and Nd of $Nd_2Ir_2O_7$ varying only U_d on Ir from 0 to 8 eV

Hubbard U (value/eV)	Lattice Constant (Å)	Magnetic moment of Ir μ_B	Magnetic moment of Nd μ_B
Exp	10.3768	0.34	2.3 ± 0.4
0	10.3140	0.01	3.33
1	10.3124	0.01	2.99
2	10.2140	0.03	2.91
3	10.2826	0.04	2.91
4	10.2755	0.11	2.90
5	10.2584	0.28	2.87
6	10.2584	0.37	2.85
7	10.2436	2.02	2.29
8	10.2115	3.10	1.90

move toward lower energy, the top of the valence band develops more O-2p character with increasing U_d. On the other hand, the Nd-f state is still more distributed near the Fermi energy. It means that the Nd-f state is unaffected by U_d on Ir, causing the band gap to close. Indicates that character with increasing only U_d on Ir correction may not be sufficient to turn $Nd_2Ir_2O_7$ metal into an insulator, in contradiction with resistivity measurements that claim that $Nd_2Ir_2O_7$ is a Mott insulator. The estimated lattice parameters and magnetic moment of Ir and Nd as a function of U_d start from U_d = 0-8 eV are shown in Table 1 compared with neutron experimental values. All calculated lattice parameters range from 10.2134 to 10.3142 Å as a function of U_d, which is lower than the lattice parameter from the experimental (10.3768 Å) [30]. However, we have the maximum percentage error of 1.57 % for U_d = 8 eV. We note an increase in the magnetic moment of the Ir atom in line with the U_d correlation for metallic $Nd_2Ir_2O_7$, from 0.01 to 3.10 μ_B. The best agreement with the neutron experimental value (0.34 μ_B) is found for U_d = 6 eV. However, for the range of U_d = 4-6 eV, the percentage error is relatively small, at less than 5.5 %, which agrees with previous reports. On the other hand, the magnetic moment of the Nd atom is in line with the d state correlation $Nd_2Ir_2O_7$ around 3.00 μ_B, which is higher than the experiment value. It means the U_d of Ir does not affect the magnetic moment of Nd. The GGA+SOC+U calculated magnetic structure of $Nd_2Ir_2O_7$ has the lowest energy and is stable in the antiferromagnetic along U_d = 0-4 eV. In contrast, the U_d = 5-8 eV has the lowest energy in the ferromagnetic phase.

3.2 $U_d = 0, U_f \neq 0$

A notable observation is the consistent endeavor to generate a band gap of $Nd_2Ir_2O_7$ from metal to be an insulator. We set U_f on only Nd atoms. U_f varied between 0 and 8 eV and influenced the energy levels of the f orbital on the Ir atom of $Nd_2Ir_2O_7$. Figure 3 illustrates the DOS of $Nd_2Ir_2O_7$ in the GGA+SOC+U approximation as a function of U_f on Nd. The GGA+SOC+U approximation showed that the O-p, Ir-d, and Nd-f states have more contributions around Fermi energy, starting from U_f = 0 eV. The Nd-f state near Fermi energy decreased around U_f = 1-3 eV, and they were spread out at U_f = 4 eV and decreased around 0.2 eV over a U_f range from 4 to 8 eV. The f orbitals show a broader distribution rather than another state. On the other hand, the strong hybridization between the transition metal

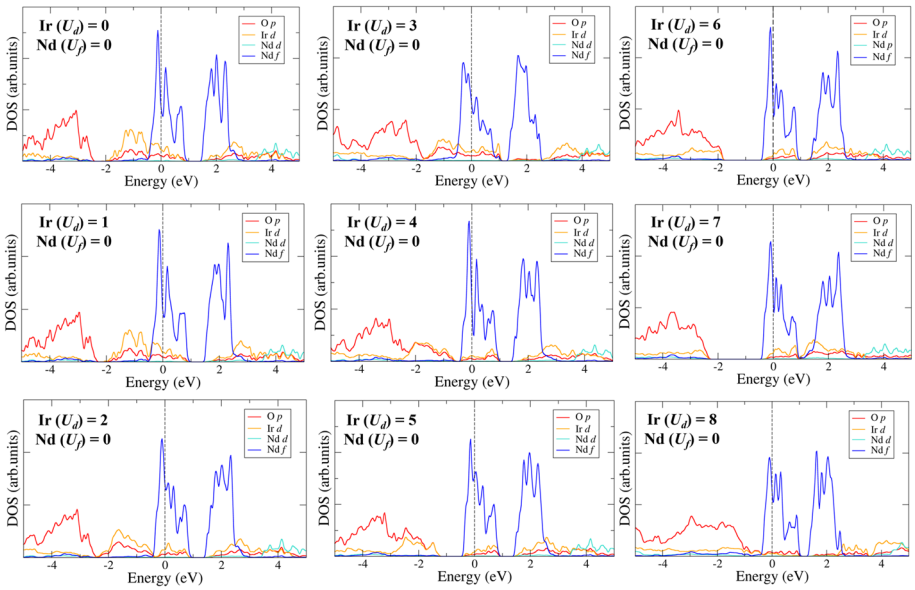

Fig. 3 PDOS (in states/eV/cell) for all materials studied in this work obtained using DFT+SOC+U with atomic projectors. The U_d correction was applied both to the d states of Ir elements. PDOS are color-coordinated such that p states of O are red, p states of Ir are yellow, d and f states of Nd are blue. The zero of energy corresponds to the top of valence bands

$5d$ electrons and the oxygen $2p$ states hinges on their relative energy positions, determining the extent of hybridization and the width of the valence band. The Occupied Ir-$5d$ and O-$2p$ still contribute near the Fermi energy with increasing U_f on Nd, unaffected by U_f on Nd, causing the band gap to close. It suggests that only the U_f correction is insufficient to induce the insulating behavior. Table 2 displays computed lattice parameters as a function of the U_f on Nd. The lattice parameter varies from 10.3141 to 10.4045 Å. These values fall below the experimental value, except for the case of U_f = 5-8 eV. The maximum percentage deviation occurs at 0.60 %. Notably, we observe an augmentation in the magnetic moment of Nd, which is 3.33 eV and decreases to 2.85 eV at U_f = 6 eV, which is still higher than the experimental value (2.3 μ_B) [19]. We observe a rise in the magnetic moment of the Ir atom, consistent with the correlation in the f states for $Nd_2Ir_2O_7$, which is 0.01 μ_B. The GGA+SOC+U calculations for the magnetic structure of $Nd_2Ir_2O_7$ reveal that the lowest energy configuration is stable in the antiferromagnetic phase within the range of U_f = 0-6 eV. Conversely, for U_f values in the range of 7-8 eV, the lowest energy configuration is found in the ferromagnetic phase Fig. 4.

3.3 $U_d \neq 0, U_f \neq 0$

The separate Hubbard U parameter to the U_d on Ir and U_f on Nd effectively rectifies the lattice parameter and magnetic moment values for Ir and Nd. However, despite these adjustments, the band gap of $Nd_2Ir_2O_7$ remains metal, consistent with the experimental value. We have adopted U_d on Ir 5 eV and varying U_f on start Nd from 5 to 8 eV. In the previous session, Ir-d and Nd-f states spread along these U to describe and discuss the electronic structure of $Nd_2Ir_2O_7$. Figure 5 presents the DOS and band structure of $Nd_2Ir_2O_7$ in the GGA+SOC+U

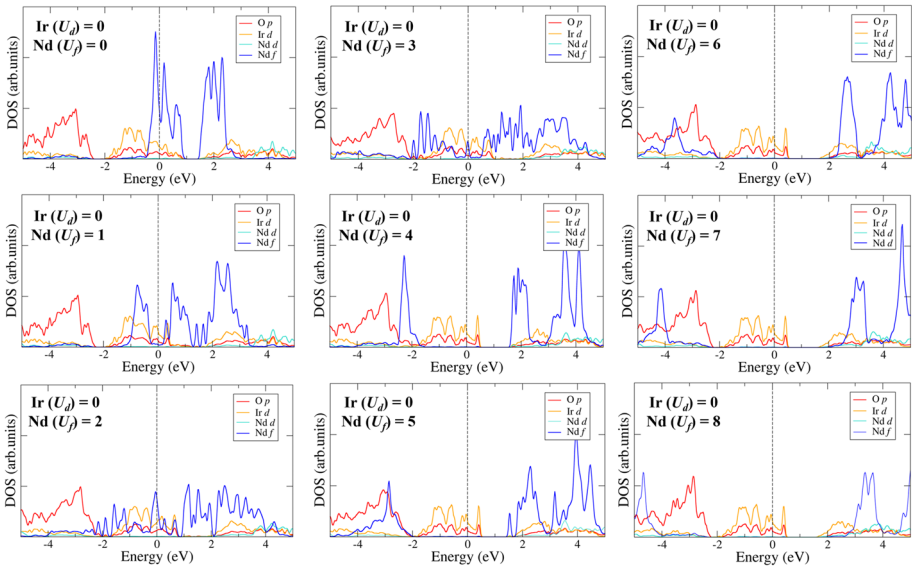

Fig. 4 PDOS (in states/eV/cell) for all materials studied in this work obtained using DFT+U_f with atomic projectors. The U_f correction was applied both to the d states of Nd elements. PDOS are color-coordinated such that p states of O are red, p states of Ir are yellow, d and f states of Nd are blue. The zero of energy corresponds to the top of valence bands

Table 2 Calculated lattice parameters (a) and magnetic moment of Ir and Nd of $Nd_2Ir_2O_7$ varying only U_f on Nd from 0 to 8 eV

Hubbard U (value/eV)	Lattice Constant (Å)	Magnetic moment of Ir μ_B	Magnetic moment of Ir μ_B
Exp	10.3768	0.34	2.3 ± 0.4
0	10.3141	0.01	2.99
1	10.3273	0.01	3.01
2	10.3559	0.01	3.01
3	10.3655	0.01	3.01
4	10.3730	0.01	3.02
5	10.3813	0.01	3.02
6	10.3903	0.01	3.02
7	10.3928	0.01	3.00
8	10.4045	0.01	3.00

approximation, we illustrate the evolution of the DOS with U_d of Ir and U_f of Nd for $Nd_2Ir_2O_7$. The GGA+SOC+U approximation considering U_d = 5 eV and U_f = 5 eV, the PDOS indicates that the valence band is mainly dominated by O-2p states, with notable localized Nd-4f lying around -1.8 eV below the top of the valence band. There is also a small contribution from Ir-5d states to most regions of the valence band. The Ir-5d constitutes most of the conduction band bottom, with the localization of Nd-4f lying around 2.8 eV. In this system, the U_f effect of the Nd-4f state shifts to the valence region by 1 eV over from U_f = 6 to 8 eV. However, considering the effective onsite Coulomb interaction both U_d on Ir and

Table 3 Calculated lattice parameters (a), band gap and magnetic moment of Ir and Nd of $Nd_2Ir_2O_7$ varying U_d on Ir and U_f on Nd

Hubbard U		Lattice constant (Å)	Band gap (eV)	Magnetic moment of Ir (μ_B)	Magnetic moment of Nd (μ_B)
U_d	U_f				
5	5	10.3841	1.58	0.32	3.00
5	6	10.3905	1.53	0.31	3.00
5	7	10.3999	1.49	0.32	3.01
5	8	10.4066	1.50	0.34	2.98
Experimental		10.3768	Metal-insulator	0.34	2.3 ± 0.4

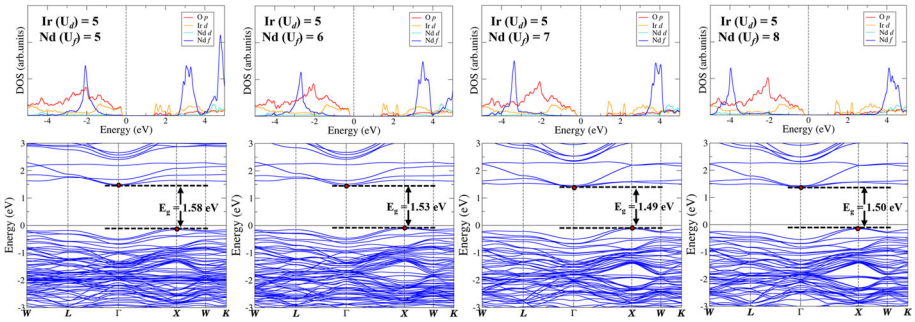

Fig. 5 Obtain the density of state and band structure of $Nd_2Ir_2O_7$ within GGA+SOC+U varying U_d on Ir and U_f on Nd. The fermi energies are set to zero

U_f on Nd can open a sizeable band gap of $Nd_2Ir_2O_7$, in our current calculation we found that U_d = 3 eV and U_f = 5 eV is on the border of the metal-insulator transition. Whereas the values of U_d = 5 eV and U_f = 5 eV open the gap around 1.58 eV in agreement with the experimental result. The band gap is indirect since the valence band maximum (VBM) occurs at the X point, and the conduction band minimum (CBM) occurs at the Γ point. The calculation lattice parameter U_d = 5 eV and U_f = 5 to 8 eV of the $Nd_2Ir_2O_7$ has a value between 10.3841 to 10.4066 Å, as shown in Table 3, which agrees with the experimental value. Indeed, we have a maximum percentage error of 0.29 % for U_d = 5 eV and U_f = 8 eV, respectively. The magnetic moment calculation of Ir for insulator $Nd_2Ir_2O_7$ is 0.31 μ_B. The best agreement with the experimental value (0.34 μ_B) is found for U_d = 5 eV and U_f = 5 eV. However, for the range of U_f = 5 to 8 eV, the percentage error is relatively small, at less than 5.5 %, which agrees with neutron diffraction experiment report [20]. We note that an increase in the Nd magnetic moment for $Nd_2Ir_2O_7$ is constant around 2.99-3.02 μ_B, higher than the experimental value (2.3 μ_B) and Crystalline field analysis [31]. The GGA+SOC+U calculations for the magnetic structure of $Nd_2Ir_2O_7$ indicate that the lowest energy configuration is stable in the ferromagnetic phase when adjusting both U_d to 5 eV and U_f in the range of 5-8 eV. Detail confirmation of the final results are still going on in order to demonstrate much more accurate values of U_f and U_d. What we can say at this stage is that both U_d and U_f of around 5 eV should be near the border of the "metal-insulator transition. Detail values will be published in a separate paper with more DFT calculation results will be published soon.

4 Conclusion

The electronic structures and magnetic properties of $Nd_2Ir_2O_7$ have been investigated using the GGA+U scheme and relativistic spin-orbit coupling (SOC). The effects of effective U values on pyrochlores structural and electronic properties have been studied. It is shown that for strongly correlated systems, correcting the intraband Coulomb interaction by the Hubbard U parameter is necessary. We suggest that the electronic structure can be reasonably described by GGA+SOC+U functional with $U_f \geq 5$ eV for Nd-4f orbital and $U_d \geq 5$ eV for Ir-5d orbital as the suitable beginning value to observe to open the band gap from metal to insulator of pyrochlore $Nd_2Ir_2O_7$. The AIAO model shows the magnetic structure of $Nd_2Ir_2O_7$ confirmed by the GGA+SOC+U calculate the spin-orbit coupling between Nd^{3+} and Ir^{4+}

moments show $Nd_2Ir_2O_7$ were stable at the ferromagnetic phase at U_d(Ir) = 5 eV, U_f(Nd) = 5, 6, 7 and 8 eV. Setting U_d on Ir and U_f on Nd are 5 and 5 eV, respectively, the estimated gap shows 1.58 eV, and the lattice parameter is 10.3841 Å, close to the experimental value. Ir^{4+} magnetic moment calculation is 0.32 μ_B, which agrees with the neutron diffraction result. On the other hand, The magnetic moment of Nd^{3+} is 3.00 μ_B higher than the experiment value. Our results can guide the calculation in the next step and support previous and future practicals.

Acknowledgements This work was supported by the International Program Associate (IPA) of RIKEN. S.C. was supported by the Graduate School of Kasetsart University. We would like to acknowledge the HOKUSAI supercomputing facility of RIKEN. We thank K. Dabsamut for the fruitful discussions.

Author Contributions Supparat Charoenphon wrote the main manuscript text and prepared all of figures. Utami Widyaiswari reviewed the manuscript. Muhammad Abdan Syakuur reviewed the manuscript. Retno Asih Pakpoom Reunchan Isao Watanabe reviewed the manuscript.

Data Availability No datasets were generated or analysed during the current study.

Declarations

Competing of interest The authors declare no competing interests.

References

1. Maiti, K.: Role of spin-orbit coupling and electron correlation in the electronic structure of a 5*d* pyrochlore, $Y_2Ir_2O_7$. Solid. State. Commun. **149**(33–34), 1351–1355 (2009)
2. Pesin, D., Balents, L.: Mott physics and band topology in materials with strong spin-orbit interaction. Nat. Phys. **6**(5), 376–381 (2010)
3. Kargarian, M., Wen, J., Fiete, G.A.: Competing exotic topological insulator phases in transition-metal oxides on the pyrochlore lattice with distortion. Phys. Rev. B **83**(16), 165112 (2011)
4. Witczak-Krempa, W., Kim, Y.B.: Topological and magnetic phases of interacting electrons in the pyrochlore iridates. Phys. Rev. B **85**(4), 045124 (2012)
5. Yang, K.-Y., Lu, Y.-M., Ran, Y.: Quantum hall effects in a weyl semimetal: Possible application in pyrochlore iridates. Phys. Rev. B **84**(7), 075129 (2011)
6. Imada, M., Fujimori, A., Tokura, Y.: Metal-insulator transitions. Rev. Mod. Phys. **70**(4), 1039 (1998)
7. Norman, M.R.: The challenge of unconventional superconductivity. Sci **332**(6026), 196–200 (2011)
8. Stewart, G.: Unconventional superconductivity. Adv. Phys. **66**(2), 75–196 (2017)
9. Fiebig, M.: Revival of the magnetoelectric effect. J. Phys. D: Appl. Phys. **38**(8), 123 (2005)
10. Fiebig, M., Lottermoser, T., Meier, D., Trassin, M.: The evolution of multiferroics. Nat. Rev. Mater. **1**(8), 1–14 (2016)
11. Wan, X., Turner, A.M., Vishwanath, A., Savrasov, S.Y.: Topological semimetal and fermi-arc surface states in the electronic structure of pyrochlore iridates. Phys. Rev. B **83**(20), 205101 (2011)
12. Talanov, M.V., Talanov, V.M.: Formation of breathing pyrochlore lattices: structural, thermodynamic and crystal chemical aspects. CrystEngComm **22**(7), 1176–1187 (2020)
13. Nakatsuji, S., Machida, Y., Maeno, Y., Tayama, T., Sakakibara, T., Van Duijn, J., Balicas, L., Millican, J., Macaluso, R., Chan, J.Y.: Metallic spin-liquid behavior of the geometrically frustrated kondo lattice $Pr_2Ir_2O_7$. Phys. Rev. Lett. **96**(8), 087204 (2006)
14. Matsuhira, K., Wakeshima, M., Hinatsu, Y., Takagi, S.: Metal-insulator transitions in pyrochlore oxides $ln_2Ir_2O_7$. J. Phys. Soc. Jpn. **80**(9), 094701 (2011)
15. Sagayama, H., Uematsu, D., Arima, T.-h., Sugimoto, K., Ishikawa, J., O'farrell, E., Nakatsuji, S.: Determination of long-range all-in-all-out ordering of ir^{4+} moments in a pyrochlore iridate $Eu_2Ir_2O_7$ by resonant x-ray diffraction. Phys. Rev. B **87**(10), 100403 (2013)
16. Yanagishima, D., Maeno, Y.: Metal-nonmetal changeover in pyrochlore iridates. J. Phys. Soc. Jpn. **70**(10), 2880–2883 (2001)

17. Ueda, K., Fujioka, J., Takahashi, Y., Suzuki, T., Ishiwata, S., Taguchi, Y., Tokura, Y.: Variation of charge dynamics in the course of metal-insulator transition for pyrochlore-type $Nd_2Ir_2O_7$. Phys. Rev. Lett. **109**(13), 136402 (2012)
18. Sakata, M., Kagayama, T., Shimizu, K., Matsuhira, K., Takagi, S., Wakeshima, M., Hinatsu, Y.: Suppression of metal-insulator transition at high pressure and pressure-induced magnetic ordering in pyrochlore oxide $Nd_2Ir_2O_7$. Phys. Rev. B **83**(4), 041102 (2011)
19. Tomiyasu, K., Matsuhira, K., Iwasa, K., Watahiki, M., Takagi, S., Wakeshima, M., Hinatsu, Y., Yokoyama, M., Ohoyama, K., Yamada, K.: Emergence of magnetic long-range order in frustrated pyrochlore $Nd_2Ir_2O_7$ with metal-insulator transition. J. Phys. Soc. Jpn. **81**(3), 034709 (2012)
20. Guo, H., Ritter, C., Komarek, A.: Direct determination of the spin structure of $Nd_2Ir_2O_7$ by means of neutron diffraction. Phys. Rev. B **94**(16), 161102 (2016)
21. Ramadhan, M.R., Adiperdana, B., Ramli, I., Sari, D.P., Putri, A.E., Widyaiswari, U., Rozak, H., Zaharim, W.N., Manaf, A., Kurniawan, B., et al.: Estimation of the on-site coulomb potential and covalent state in La_2CuO_4 by muon spin rotation and density functional theory calculations. Phys. Rev. Res **4**(3), 033044 (2022)
22. Varnava, N., Vanderbilt, D.: Surfaces of axion insulators. Phys. Rev. B **98**(24), 245117 (2018)
23. Laguna-Marco, M., Kayser, P., Alonso, J., Martínez-Lope, M., Van Veenendaal, M., Choi, Y., Haskel, D.: Electronic structure, local magnetism, and spin-orbit effects of ir (iv)-, ir (v)-, and ir (vi)-based compounds. Phys. Rev. B **91**(21), 214433 (2015)
24. Antonov, V., Bekenov, L., Kukusta, D.: Pyrochlore iridates: Electronic and magnetic structures, x-ray magnetic circular dichroism, and resonant inelastic x-ray scattering. Phys. Rev. B **102**(19), 195134 (2020)
25. Asih, R., Adam, N., Mohd-Tajudin, S.S., Sari, D.P., Matsuhira, K., Guo, H., Wakeshima, M., Hinatsu, Y., Nakano, T., Nozue, Y., et al.: Magnetic moments and ordered states in pyrochlore iridates $Nd_2Ir_2O_7$ and $Sm_2Ir_2O_7$ studied by muon-spin relaxation. J. Phys. Soc. Jpn. **86**(2), 024705 (2017)
26. Perdew, J.P., Chevary, J.A., Vosko, S.H., Jackson, K.A., Pederson, M.R., Singh, D.J., Fiolhais, C.: Atoms, molecules, solids, and surfaces: Applications of the generalized gradient approximation for exchange and correlation. Phys. Rev. B **46**(11), 6671 (1992)
27. Shishkin, M., Sato, H.: DFT + U in dudarev's formulation with corrected interactions between the electrons with opposite spins: The form of hamiltonian, calculation of forces, and bandgap adjustments. Chem. Phys. 151(2) (2019)
28. Hagiwara, T., Nomura, K., Kageyama, H.: Crystal structure analysis of $ln_2Zr_2O_7$ (ln = eu and la) with a pyrochlore composition by high-temperature powder x-ray diffraction. J. Ceram. Soc. Jpn. **125**(2), 65–70 (2017)
29. Setyawan, W., Curtarolo, S.: High-throughput electronic band structure calculations: Challenges and tools. Comput. Mater. Sci. **49**(2), 299–312 (2010)
30. Takatsu, H., Watanabe, K., Goto, K., Kadowaki, H.: Comparative study of low-temperature x-ray diffraction experiments on $R_2Ir_2O_7$ (R = Nd, Eu, and Pr). Phys. Rev. B **90**(23), 235110 (2014)
31. Watahiki, M., Tomiyasu, K., Matsuhira, K., Iwasa, K., Yokoyama, M., Takagi, S., Wakeshima, M., Hinatsu, Y.: Crystalline electric field study in the pyrochlore $Nd_2Ir_2O_7$ with metal-insulator transition. In: Journal of physics: conference series, vol. 320, pp. 012080 (2011). IOP Publishing

Publisher's Note Springer Nature remains neutral with regard to jurisdictional claims in published maps and institutional affiliations.

Springer Nature or its licensor (e.g. a society or other partner) holds exclusive rights to this article under a publishing agreement with the author(s) or other rightsholder(s); author self-archiving of the accepted manuscript version of this article is solely governed by the terms of such publishing agreement and applicable law.